Optics Letters

Few-cycle near-infrared pulses from a degenerate 1 GHz optical parametric oscillator

Richard A. McCracken* and Derryck T. Reid

Scottish Universities Physics Alliance (SUPA), Institute of Photonics and Quantum Sciences, School of Engineering and Physical Sciences, Heriot-Watt University, Riccarton, Edinburgh EH14 4AS, UK
**Corresponding author: r.a.mccracken@hw.ac.uk*

Received 19 June 2015; revised 5 August 2015; accepted 9 August 2015; posted 11 August 2015 (Doc. ID 243046); published 27 August 2015

We report the generation of transform-limited 4.3-cycle (23 fs) pulses at 1.6 μm from a degenerate doubly resonant optical parametric oscillator (OPO) pumped by a 1 GHz mode-locked Ti:sapphire laser. A $\chi^{(2)}$ nonlinear envelope equation was used to inform the experimental implementation of intracavity group-delay dispersion compensation, resulting in resonant pulses with a 169 nm full width half-maximum spectral bandwidth, close to the bandwidth predicted by theory.

OCIS codes: (190.4410) Nonlinear optics, parametric processes; (190.4970) Parametric oscillators and amplifiers; (190.7110) Ultrafast nonlinear optics.

http://dx.doi.org/10.1364/OL.40.004102

High-repetition-rate ultrafast lasers providing broadband frequency combs with an easily resolvable mode structure are needed for astronomical spectrograph calibration [1], high-resolution direct comb spectroscopy [2], and asynchronous optical sampling [3]. Achieving short, broadband pulses while extending operation to higher repetition frequencies remains particularly challenging, because the peak powers available to drive bandwidth-enhancing $\chi^{(2)}$ and $\chi^{(3)}$ nonlinear effects are reduced as the pulse repetition rate increases. With careful dispersion management, Ti:sapphire laser oscillators have been demonstrated which directly provide few-cycle pulses at gigahertz (GHz) rates [4], but the extension of this approach to the near-infrared region has been limited by the availability of suitable broadband and low-dispersion gain media [5–7].

In this context, optical parametric oscillators (OPOs) are a promising way forward to generate broadband and high-repetition-rate pulses in the near- and even mid-infrared. They can produce frequency combs with multi-octave spectral coverage [8] and with carrier-envelope-offset frequency linewidths of a few hertz [9]. Operation at GHz rates has been reported in both synchronous [10–12] and harmonic [13,14] pumping schemes, and when stabilized to form a comb the OPO modes can be further filtered in a Fabry–Perot cavity [15] to provide >10 GHz mode spacings that can be resolved using standard optical spectrometers.

Doubly resonant OPOs [16] operated at degeneracy are a special class of synchronously pumped OPOs which combine high gain operation with an exceptionally broad oscillation bandwidth. These devices can produce a broadband frequency comb [17,18] that is centered at twice the pump wavelength and whose comb dynamics are intrinsically locked to those of the pump laser, with few-cycle pulses being demonstrated at a number of mid-infrared wavelengths [19–21]. Recently, a degenerate periodically-poled lithium niobate (PPLN) OPO pumped by a 1 GHz Ti:sapphire laser was reported which achieved an 85 nm bandwidth centered at 1.6 μm, capable of supporting sub-50 fs pulses [22]. Here we introduce a 1 GHz doubly resonant degenerate OPO based on a Brewster-cut periodically-poled potassium titanyl phosphate (PPKTP) crystal, the first synchronously pumped OPO to be demonstrated using such a crystal. The exceptional gain bandwidth of PPKTP allows this OPO to support a resonant pulse with twice the frequency bandwidth of the pump pulses, corresponding to 23 fs (4.3 cycle) pulses with a full width at half maximum (FWHM) bandwidth of 169 nm.

Despite its lower d_{33} nonlinear coefficient, PPKTP offers a number of practical advantages over MgO:PPLN in the specific context of femtosecond OPOs. Its lower refractive index means that its nonlinear figure of merit is in fact very similar to that of lithium niobate, while providing lower material dispersion than MgO:PPLN at 1.6 μm (23 $fs^2\,mm^{-1}$ for PPKTP [23]; 83 $fs^2\,mm^{-1}$ for MgO:PPLN [24]). This dispersion characteristic is evident in Fig. 1, which presents a comparison of the phase-matching bandwidth available using the MgO:PPLN crystal in [22] and the Brewster-cut PPKTP crystal which we employ here. Using a phase-matching efficiency of 50% as a reference level, the 1 mm long PPLN crystal has a phase-matching bandwidth of 500 nm.

In contrast, the 0.6 mm long PPKTP crystal—the effective path length for a beam entering a 0.5 mm crystal at Brewster's angle—has an exploitable bandwidth of 1000 nm, which is a substantial improvement. Achieving an equivalent bandwidth in MgO:PPLN would require a crystal thicknesses of <350 μm, which would have lower gain than the equivalent PPKTP crystal and would also present acute fabrication and handling challenges.

To better understand the behavior of our PPKTP OPO we employed the recently developed $\chi^{(2)}$ nonlinear envelope

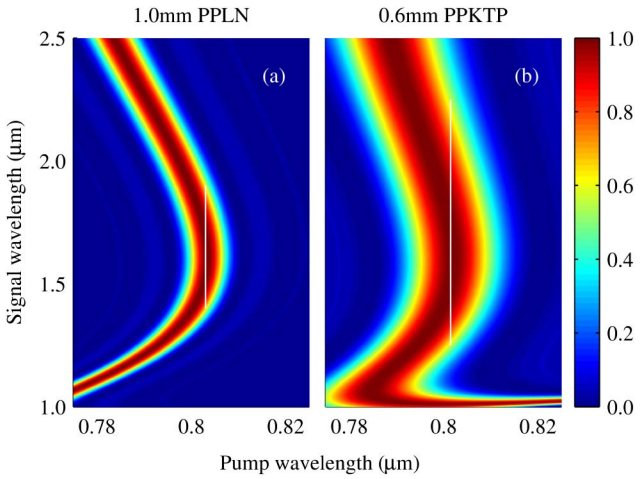

Fig. 1. Phase-matching diagrams for (a) 1.0 mm of PPLN [21] and (b) 0.6 mm of PPKTP. White lines indicate phase-matching efficiencies of >50% and are drawn as a visual guide. The color scale corresponds to $\mathrm{sinc}^2(\Delta kL/2)$, which is a direct measure of the phase-matching efficiency.

equation (NEE) model [25], which has previously been used to study ultrabroadband pulse evolution in both singly and doubly resonant OPOs [26]. In Fig. 2 we show the evolution of the OPO intracavity intensity as it builds up from a weak seed pulse. A steady-state condition is reached after around 100 round trips. The round trip cavity reflectivity, physically based on an appropriate quarter-wave Bragg-mirror coating, is shown for comparison and implies that the OPO bandwidth is limited in practice by the reflectivity of this mirror and its associated dispersion. The round trip intracavity loss was chosen to match the combined experimental loss and output coupling of 30%, and the pump intensity was selected to be 2.3× the threshold intensity, again to match the experimental conditions. Under these criteria the pump intensity used in the model was also

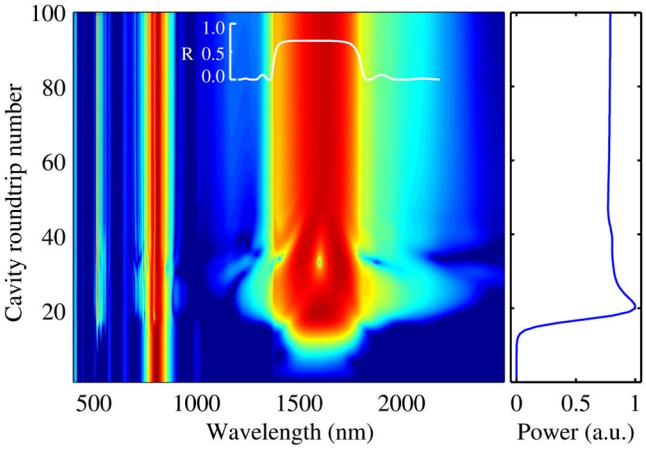

Fig. 2. Left: color-map representation of the intensity of the participating intracavity pulses as the OPO builds up to a steady-state condition after approximately 100 round trips, with the main fields being the pump + OPO sum-frequency light near 500 nm, the pump at 800 nm, and the OPO around 1600 nm. The round trip cavity reflectivity used in the model is represented in white. Right: power contained in the OPO field, evaluated in the range of 1000–2000 nm.

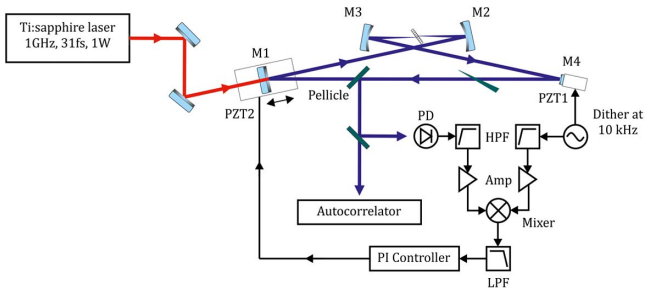

Fig. 3. Optical and electronic layout of the degenerate 1 GHz PPKTP OPO. HPF, high-pass filter; LPF, low-pass filter; PD, photodiode; PZT, piezoelectric transducer.

found to be very close to the experimental value, within limits of the uncertainty associated with knowing the exact spot size and peak power inside the PPKTP crystal.

The experimental layout is shown in Fig. 3. The pump source for the OPO was a 1 GHz Ti:sapphire laser (Gigajet, Laser Quantum) which produced 31 fs $\mathrm{sech}^2(t)$ pulses centered at 803 nm. The OPO was synchronously pumped by the Ti:sapphire laser, such that their cavity lengths (~300 mm) were equal. The OPO was a 4-mirror ring cavity based around a 0.5 mm length of PPKTP with a domain period of 26.5 μm (Raicol Crystals) cut at Brewster's angle of 1.6 μm. Pump light was coupled into the cavity through mirror M1 which was mounted on a translation stage for coarse cavity length adjustments. A pair of curved mirrors with 20 mm radius of curvature (M2 and M3) was chosen such that a $1/e^2$ waist size of 14.1 μm was achieved in the crystal. The folding angle of the curved mirrors was 6°, allowing for compensation of the astigmatism introduced by the Brewster-angled crystal. Mirror M4 was mounted on a piezoelectric transducer (PZT1) used for dither-locking the cavity. Mirror M2 was silver coated, allowing the pump beam to be focused directly into the crystal without using a lens. The remaining OPO cavity mirrors had a dielectric coating which transmitted the pump light and were highly reflective ($R > 99.9\%$) over the 1400–1800 nm region.

Figure 4 shows the output power of the OPO as the cavity length was scanned over a range of several pump wavelengths using PZT2, a long travel piezo attached to the translation

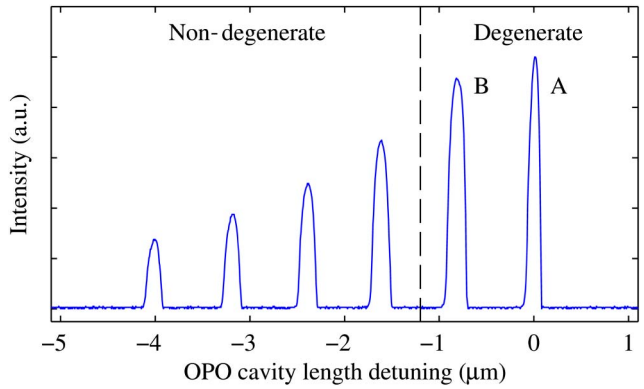

Fig. 4. Output power of the OPO as the cavity length was scanned. The spacing between oscillation peaks corresponds to one pump wavelength. While both peaks A and B were found to be degenerate, the broadest bandwidth was obtainable from peak B.

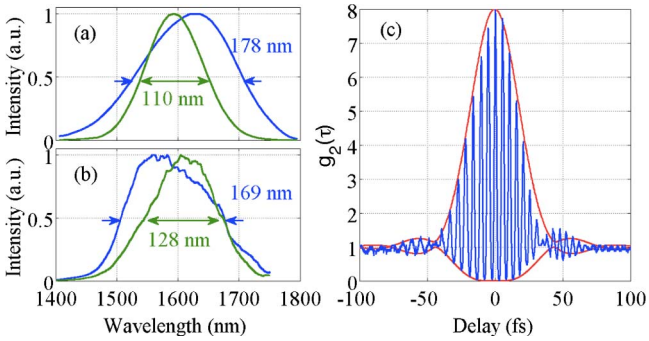

Fig. 5. (a) Modeled spectra of the OPO operated without (green) and with (blue) a 1 mm fused-silica intracavity wedge. (b) Experimental spectra obtained without (green) and with (blue) an intracavity fused-silica wedge. (c) Two-photon autocorrelation of the OPO pulses generated using the intracavity fused-silica wedge. The red line shows the autocorrelation envelope derived by Fourier transforming the blue spectrum in (b), illustrating that the pulses are transform-limited directly from the OPO cavity. Full width half-maximum bandwidths are shown in (a) and (b).

stage beneath mirror M1. Unlike previously reported degenerate OPOs based on MgO:PPLN, no passive thermal locking of the cavity was observed, which can be explained by MgO:PPLN having a larger thermo-optic coefficient (dn_e/dT) than PPKTP. In order to stabilize the OPO, we employed a dither-and-lock approach. A low amplitude 10 kHz dither was applied to PZT1 while a slow scan of the cavity length was introduced via PZT2. A pellicle beam splitter (Thorlabs BP545B3) was used to output couple 28% of the intracavity power, a small portion of which was directed to an InGaAs photodiode. Both the photodiode signal and dither signal were high-pass filtered before being amplified and passed to a mixer. The mixed signal was low-pass filtered and used as the input signal for a servo controller, the output of which was used to control PZT2. The 10 kHz dither frequency was chosen to be below the resonant frequency of PZT1, yet still high enough to be cleanly decoupled from the servo locking loop, which had a bandwidth of 30 Hz. Using this technique the OPO could be locked to the peak of any fringe shown in Fig. 4, with locking maintainable for several hours. The oscillation peaks labeled A and B correspond to degenerate operation, with the remaining peaks found to be either partially- or non-degenerate. Approximately 270 mW of signal power at peak B was extracted with 950 mW of incident pump power. The threshold of operation was 27 mW, which increased to 350 mW when the output coupler was in place.

With no intracavity dispersion compensation the FWHM bandwidth of the signal pulses was 128 nm, which is capable of supporting 30 fs Gaussian pulses. Following modeling which indicated that broader bandwidths would be achieved with intracavity dispersion compensation, a 1 mm fused silica wedge was introduced into the cavity in order to compensate for the positive material dispersion of the PPKTP crystal, resulting in a bandwidth of 169 nm. Modeled and experimental spectra from the degenerate OPO are shown in Figs. 5(a) and 5(b), respectively. The slight center wavelength deviation between the modeling and experimental results arises due to the sensitivity of the NEE model to the OPO mirror reflectivity, which has a ±20 nm uncertainty at the wavelength extremes.

A two-photon autocorrelation of the OPO pulses generated using the intracavity fused-silica wedge is shown in Fig. 5(c). Fourier-transforming the spectrum of the pulses and fitting to the autocorrelation trace reveals transform-limited 23 fs Gaussian pulses, corresponding to 4.3 optical cycles at 1.6 μm. The NEE model suggests that a bandwidth of 178 nm is achievable, and we attribute this small discrepancy to an uncertainty in the insertion length of the fused silica wedge, combined with imperfect rendering of the exact mirror reflectivity and dispersion properties in the model.

In conclusion, we have demonstrated a degenerate synchronously pumped 1 GHz OPO which can produce few-cycle 23 fs pulses centered around 1.6 μm and with a FWHM bandwidth of 169 nm. By careful management of the intracavity dispersion and reflectivity we expect this bandwidth could be extended considerably further, since the theoretical gain spectrum of PPKTP in this configuration can support near-octave-spanning pulses. With intrinsic phase locking to the pump laser, such an OPO represents a promising source for ultrabroadband, mode-resolvable near-IR frequency combs, offering the spectral coverage of Er:fiber technology but with the capability to generate multi-GHz combs (using multi-GHz Ti:sapphire pump lasers) without the need for Fabry–Perot filtering. Furthermore, the high peak powers (~8 kW) and extremely short durations of the pulses generated from the OPO should mean that supercontinuum generation will be possible using only a few cm of suitable fiber and will evolve in a way that fully maintains the coherence of the original pulses across a bandwidth of many hundreds of nanometers.

Funding. Science and Technology Facilities Council (STFC) (ST/L002140/1).

Acknowledgment. We thank Gamdan Optics Inc. for Brewster-angled cutting of the PPKTP crystal. We also thank Alireza Marandi, Kirk A. Ingold, and Robert L. Byer at Stanford University for their discussions regarding degenerate OPOs. RAM is grateful for travel funding under the SU2P staff exchange program.

REFERENCES

1. D. F. Phillips, A. G. Glenday, C.-H. Li, C. Cramer, G. Furesz, G. Chang, A. J. Benedick, L.-J. Chen, F. X. Kärtner, S. Korzennik, D. Sasselov, A. Szentgyorgyi, and R. L. Walsworth, Opt. Express **20**, 13711 (2012).
2. S. A. Diddams, L. Hollberg, and V. Mbele, Nature **445**, 627 (2007).
3. A. Bartels, R. Cerna, C. Kistner, A. Thoma, F. Hudert, C. Janke, and T. Dekorsy, Rev. Sci. Instrum. **78**, 035107 (2007).
4. Y. Kobayashi, D. Yoshitomi, K. Torizuka, T. Fortier, and S. Diddams, "Sub 6-fs pulses generated from a broadband 1-GHz Ti:sapphire oscillator," in *Conference on Lasers and Electro-Optics (CLEO)*, May 2007, paper CTuC3.
5. H.-W. Chen, G. Chang, S. Xu, Z. Yang, and F. X. Kärtner, Opt. Lett. **37**, 3522 (2012).
6. D. Chao, M. Y. Sander, G. Chang, J. L. Morse, J. A. Cox, G. S. Petrich, L. A. Kolodziejski, F. X. Kärtner, and E. P. Ippen, "Self-referenced erbium fiber laser frequency comb at a GHz repetition rate," in *Optical Fiber Communication Conference (OFC)*, March 2012, paper OW1C.2.
7. A. E. H. Oehler, T. Südmeyer, K. J. Weingarten, and U. Keller, Opt. Express **16**, 21930 (2008).

8. J. H. Sun, B. J. S. Gale, and D. T. Reid, Opt. Lett. **32**, 1414 (2007).
9. T. I. Ferreiro, J. Sun, and D. T. Reid, Opt. Express **19**, 24159 (2011).
10. X. P. Zhang, J. Hebling, A. Bartels, D. Nau, J. Kuhl, W. W. Rühle, and H. Giessen, Appl. Phys. Lett. **80**, 1873 (2002).
11. R. Gebs, T. Dekorsy, S. A. Diddams, and A. Bartels, Opt. Express **16**, 5397 (2008).
12. R. A. McCracken, K. Balskus, Z. Zhang, and D. T. Reid, Opt. Express **23**, 16466 (2015).
13. K. Balskus, S. M. Leitch, Z. Zhang, R. A. McCracken, and D. T. Reid, Opt. Express **23**, 1283 (2015).
14. O. Kokabee, A. Esteban-Martin, and M. Ebrahim-Zadeh, Opt. Express **17**, 15635 (2009).
15. Z. Zhang, K. Balskus, R. A. McCracken, and D. T. Reid, Opt. Lett. **40**, 2692 (2015).
16. S. T. Wong, T. Plettner, K. L. Vodopyanov, K. Urbanek, M. Digonnet, and R. L. Byer, Opt. Lett. **33**, 1896 (2008).
17. N. Leindecker, A. Marandi, R. L. Byer, and K. L. Vodopyanov, Opt. Express **19**, 6296 (2011).
18. N. Leindecker, A. Marandi, R. L. Byer, K. L. Vodopyanov, I. Hartl, M. Fermann, P. G. Schunemann, J. Jiang, I. Hartl, M. Fermann, and P. G. Schunemann, Opt. Express **20**, 7046 (2012).
19. M. W. Haakestad, A. Marandi, N. Leindecker, and K. L. Vodopyanov, Laser Photon. Rev. **7**, L93 (2013).
20. C. W. Rudy, A. Marandi, K. A. Ingold, S. J. Wolf, K. L. Vodopyanov, R. L. Byer, L. Yang, P. Wan, and J. Liu, Opt. Express **20**, 27589 (2012).
21. S. Chaitanya Kumar, A. Esteban-Martin, T. Ideguchi, M. Yan, S. Holzner, T. W. Hänsch, N. Picqué, and M. Ebrahim-Zadeh, Laser Photon. Rev. **8**, L86 (2014).
22. M. Vainio, M. Merimaa, L. Halonen, and K. Vodopyanov, Opt. Lett. **37**, 4561 (2012).
23. K. Fradkin, A. Arie, A. Skliar, and G. Rosenman, Appl. Phys. Lett. **74**, 914 (1999).
24. D. E. Zelmon, D. L. Small, and D. Jundt, J. Opt. Soc. Am. B **14**, 3319 (1997).
25. M. Conforti, F. Baronio, and C. De Angelis, Phys. Rev. A **81**, 053841 (2010).
26. D. T. Reid, Opt. Express **19**, 17979 (2011).